Nano Energy 54 (2018) 453–460

Contents lists available at ScienceDirect

Nano Energy

journal homepage: www.elsevier.com/locate/nanoen

Full paper

Rotation sensing and gesture control of a robot joint via triboelectric quantization sensor

Xianjie Pu[a,1], Hengyu Guo[a,b,c,1], Qian Tang[a,1], Jie Chen[a], Li Feng[a], Guanlin Liu[a,c], Xue Wang[a], Yi Xi[a], Chenguo Hu[a,*], Zhong Lin Wang[b,c,**]

[a] Department of Applied Physics, State Key Laboratory of Power Transmission Equipment & System Security and New Technology, Chongqing University, Chongqing 400044, PR China

[b] Beijing Institute of Nanoenergy and Nanosystems, Chinese Academy of Sciences, Beijing 100083, PR China

[c] School of Materials Science and Engineering, Georgia Institute of Technology, Atlanta, GA 30332-0245, USA

ARTICLE INFO

Keywords:
Human-machine interface
Robotic hand control
Joint motion sensor
Triboelectric nanogenerator
Hand gesture

ABSTRACT

In human-machine interaction, robotic hands are expected to work like human's hands and to be even more powerful or delicate in certain situations. To operate robotic hands via human gesture instead of handle or button will make this human-robot interface more natural and precise. Here, we designed a joint motion triboelectric quantization sensor (jmTQS) for constructing a robotic hand synchronous control system. Based on the ultrahigh sensitivity of a triboelectric nanogenerator (TENG) to mechanical displacement, the jmTQS designed as grating-sliding mode realized directly quantifying a joint's flexion-extension degree/speed. Through counting the pulses induced by jmTQS and signing the positive/negative of the pulses to represent flexion/extension, the joint's angular position can be determined with absolute value on the basis of the initial human-robotic synchronizing position value. In the whole operating course, the intuitionistic human-robotic hand two-dimensional motion mapping can be preserved. The minimum resolution angle of the fabricated jmTQSs is 3.8° and can be further improved by decreasing the grating width. This direct quantization and intuitionistic mapping at the sensing stage greatly simplified the signal processing and classification algorithms, which contributes to achieving the natural, high-precision and real-time interface.

1. Introduction

Robotics has been developing rapidly in recent years. Human-robot cooperation has fundamentally changed the traditional industrial production, enabling mankind to enter the era of intelligence from manual operation, mechanization and automation. Robots are not only widely used in manufacturing industry, but also have played an important role in extreme environments such as deep-sea exploration, aerospace application, military operation and disaster salvation etc [1,2]. In these remote operation environments, robotic hands are expected to work as dexterous as human's hands, or to be even more powerful or delicate than human hands. The current technologies for operating robotic hands via human gesture sensing include visual tracking [3–5], physiological signal collection [6,7] and mechanical signal collection [8–11] etc. Among these technologies, visual tracking has poor wearability due to the additional camera/lighting devices for gesture capturing and needs to study various algorithms to improve the accuracy and speed of pattern recognition in image processing [3–5]. Physiological signal used in this domain mainly focuses on electromyogram (EMG) collection and its combination with epidermal electronics technology [6,7]. This kind of integration improved wearability but was still affected by poor signal-to-noise ratio (SNR) because of the basic principle of physiological signal acquisition. For converting mechanical agitation into functional signals, the techniques of mechanomyography (MMG, based on pressure sensors etc.) [8,9], inertial measurement unit (IMU , composed of accelerometers, gyroscopes, magnetometers, etc.) [10] and force-sensitive resistor (FSR) [11] are usually adopted. In these methods, both MMG and IMU lack an intuitive correspondence between the finger movement and the output signal and therefore need to develop complex algorithms, such as fuzzy logic, support vector

* Corresponding author at: Department of Applied Physics, State Key Laboratory of Power Transmission Equipment & System Security and New Technology, Chongqing University, Chongqing 400044, PR China.

** Corresponding author at: Beijing Institute of Nanoenergy and Nanosystems, Chinese Academy of Sciences, Beijing 100083, PR China.

E-mail addresses: hucg@cqu.edu.cn (C. Hu), zhong.wang@mse.gatech.edu (Z.L. Wang).

[1] Authors with equal contribution.

https://doi.org/10.1016/j.nanoen.2018.10.044
Received 9 September 2018; Received in revised form 4 October 2018; Accepted 20 October 2018
Available online 24 October 2018

machines, and decision trees etc. to classify the output signals [9]. As to FSR, nonlinearity remains the most prominent problem. Advancing the state of the art in this domain requires a new kind of hand gesture sensor to reduce the system complexity, increase the signal amplitude, and make the algorithm simple and practical.

In recent years, the fast development of material science and technology has provided several kinds of possible strategies [12,13], e.g. the epidermal electronics as mentioned above to improve the physiological monitoring [14–16], the stretchable polymer semiconductor films as a finger-wearable driver for an LED [17], the piezoelectric nanodevices for gesture recognition [18], and applications of triboelectric nanogenerator (TENG) as a hand movement detection sensor [19–23]. Among these technologies, TENG, based on the coupling of triboelectrification and electrostatic induction, has been developed quickly as a new electromechanical conversion technology and been applied in energy harvesting and self-powered mechanical sensing [24–29]. With its unique advantage of ultrahigh sensitivity to mechanical stimulus, TENG has been used in human-machine interface to detect the micro motion caused by eye-blink as instructions [30]. Furthermore, a frequency adjustable triboelectric auditory sensor has been designed for robotics application and hearing aids [31]. These works indicated a great potential and applicability of TENG in human-machine interface as eye-movement control, verbal communication, or gesture interfaces etc. Current studies applying TENG in gesture sensing usually have the similar pattern of qualitative analysis judgment rather than quantitative analysis. For example, the TENG sensor producing a qualitative peak can only indicate a finger's bending while not sensing its bending degree [19,20] and thus cannot be used in synchronous control of robotic hand. To judge the bending degree via the signal amplitude cannot always quantify accurately because there are too many factors affecting the amplitude that will be different in each measurement [21,22]. Therefore, to control a robotic hand via gesture sensing, a finger-wearable sensor [32] that could quantitatively detect the finger's flexion-extension degree/speed is expected.

Inspired by the TENG based angle measurement sensor [33] and micro-grated linear motion sensor [34,35], we employed a hinge model [36] to verify the linear relationship between the rotation angle and the tensile displacement at the finger joint and designed and fabricated a joint motion triboelectric quantization sensor (jmTQS) to be worn on the finger to accurately detect the flexion-extension degree/speed of the target joint by counting the pulse number in unit time and signing the positive/negative peak representing flexion/extension. Hence, the finger joint's angular position can be fixed by absolute value and the intuitionistic motion-signal mapping can be set up. Consequently, the signal processing and classification algorithms can be greatly simplified for achieving the natural, high-precision and real-time interface.

2. Experimental section

2.1. Fabrication of the triboelectric sensor

The fabrication process of jmTQS can be divided into the preparation of the electrode part and slider part, and the assembling of the device. Typically, an acrylic sheet (thickness: 1 mm) was cut into a designed structure to act as the substrate as shown in Fig. S1. Then, the copper electrode pattern (thickness: 200 nm) was deposited on the surface by vacuum magnetron sputtering. Later, a surface nanostructure modified FEP film (thickness: 25 μm) was adhered onto the copper electrode to work as the tribo-layer before being fixed with two acrylic strips to form the slide way. For the sliding part, sponge foam (thickness: 1 mm) was chosen as the substrate in order to form a better contact with electrode part. Then, mask paper was stuck on the substrate and cut with the designed pattern (Fig. S2) before depositing a 200 nm copper layer. After peeling off some specific paper, the copper patterned slider was achieved. Lastly, the sliding part was connected with a PET belt and assembled with the electrode part.

2.2. Electric measurement and characterization

Field emission scanning electron microscopy (Hitachi SU8010) was used to characterize the surface morphology of the nanostructured FEP film. For the electric signal measurement of the TENG based jmTQS sensor, a home-made hinge component was employed to simulate the motion of the finger joint. A numerical controlled electric stepping motor was used to drive the hinge component to operate the device. A programmable electrometer (Keithley 6514) was adopted to measure the voltage signal. NI-6259 (National Instruments Corporation) was used for data collecting. The software platform was constructed based on LabVIEW for realizing real-time data acquisition, analysis and control.

2.3. Verification of the hinge experimental model

A piece of movable fine line was fixed along the surface of the finger's PIP joint. On the fine line, a marker was adhered to mark the displacement induced by the joint's flexion. When PIP was flexing, the subject should keep metacarpophalangeal joint (MCP) steady. The stable sliding of the marker during the joint's flexion was recorded by a digital camera (Nikon D7000). Then, the video was imported into Tacker (the Open Source Physics), in which the objects can be tracked and the displacement of the marker and the rotation angle of the finger's intermediate phalanges can be calibrated.

3. Results and discussion

3.1. Structure of the TENG sensor

To realize the pulse number counting, the grating-sliding mode is adopted as the main structure, as illustrated in Fig. 1. Fig. 1a presents the structural scheme of the jmTQS which consists of an acrylic rectangular cavity and a slider. The acrylic rectangular cavity is formed with an acrylic substrate, two acrylic spacers, and an acrylic roof covered with a metal shielding layer for better signals. A patterned copper layer is deposited on the surface of the acrylic substrate as the electrodes for generating pulse signals. Detailed components of the copper layer electrodes are shown in Fig. 1b. The copper layer is separated into two pairs of interdigital electrodes (specified by dark yellow and pale yellow). Each electrode is composed of the finer gratings (left part) and the blocks (right part). The operating principle will be described later in Fig. 3. Covering the copper electrodes, the fluorinated ethylene propylene (FEP) thin film serves as one electrification layer. Inset is the scanning electron microscopy (SEM) image of FEP film. The opposite electrification layer is the copper gratings-block in the same periodicity deposited on the sponge foam surface of the slider (as illustrated in Fig. 1b). Several belts of velcro adhered on the back of the acrylic substrate help fixing the sensor on the joint of a finger. Fig. 1c shows the as-fabricated jmTQS worn on an adult's index finger. Detailed fabrication process of the device is presented in the Experimental Section and Supporting Information (Fig. S1 and Fig. S2).

3.2. The hinge model

The joint's grating linear motion sensor described above is designed on the hypothesis that the tensile displacement at the joint during finger's flexion/extension is linear with the rotation angle. To verify this hypothesis, a theoretical hinge model to simulate the rotation around the center of the proximal interphalangeal joint (PIP) while finger's flexion/extension is proposed based on the skeleton of human finger (refer to Fig. 2a–b) [36,37]. Then, the hinge model is verified by an experimental model and its testing data (shown in Fig. 2c–d). The experimental model is tested via a digital camera (Nikon D7000, Nikon Corporation) and video analysis software (Tracker, Open Source Physics). Detailed experimental process is described in the Experimental

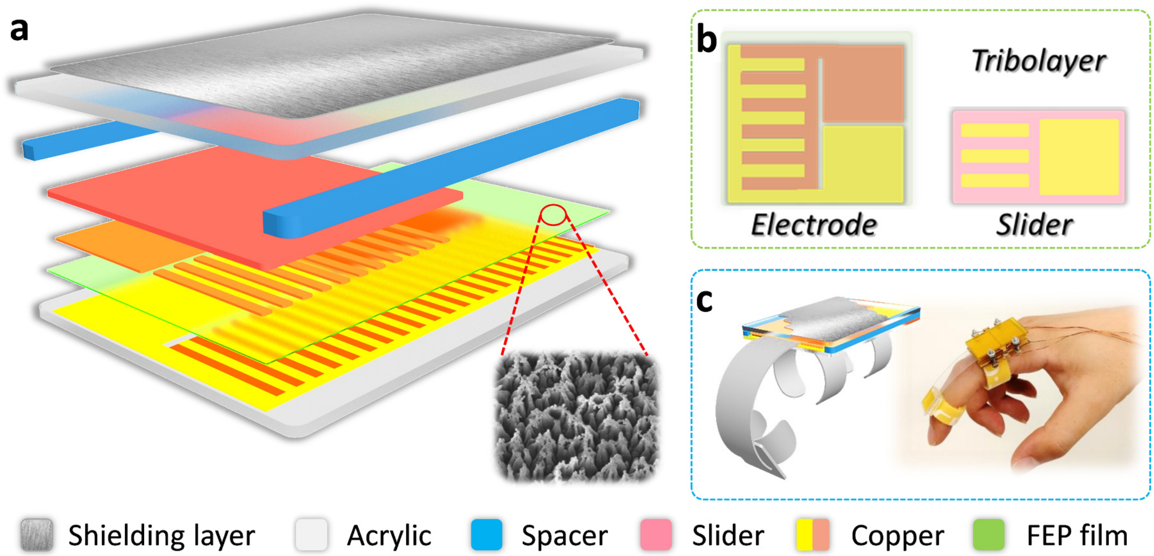

Fig. 1. Structure of the jmTQS. (a) Multilayer structure of the jmTQS. Inset: An SEM image of FEP nanowires. (b) The grating-block coupled structure on the electrode and the slider. (c) Left: jmTQS with the fixing device for convenient adjustment. Right: Photograph of an as-fabricated sensor.

Section.

3.3. Operating mechanism of the jmTQS sensor

On the basis of verified hinge model, the as-fabricated jmTQS worn on a finger joint is capable of translating the finger's flexion/extension to corresponding positive/negative pulse signal. The operating mechanism of the jmTQS is illustrated in Fig. 3. As shown in Fig. 3a and Fig. 3b, the gratings (left part) and the blocks (right part) form a coupled freestanding mode. When the slider slides forward/backward (induced by finger's flexion/extension), the relative displacement between slider and two interdigitated electrodes (dark yellow and pale yellow) leads to periodic separation from one electrode and corresponding contact to the other electrode. Due to the coupling of contact electrification and inplane displacement induced charge transfer, the alternating electric signal between the two interdigital electrodes can be detected. For the fine grating part, the alternating electric signal is a series of periodic narrow pulses while for the block part, the alternating electric signal is a wide-pulse signal. These two signals are coupled to the signal shown in Fig. 3c, thus a series of positive/negative pulses representing the finger's flexion/extension is obtained. To elucidate the working principle, the potential distribution of the gratings part (top, Fig. 3d-f) and the block part (bottom, Fig. 3d-f) under open-circuit condition are simulated by COMSOL in three phases of an ordinary cycle. Furthermore, the grating part and block part have been fabricated individually to verify the working principle by practical

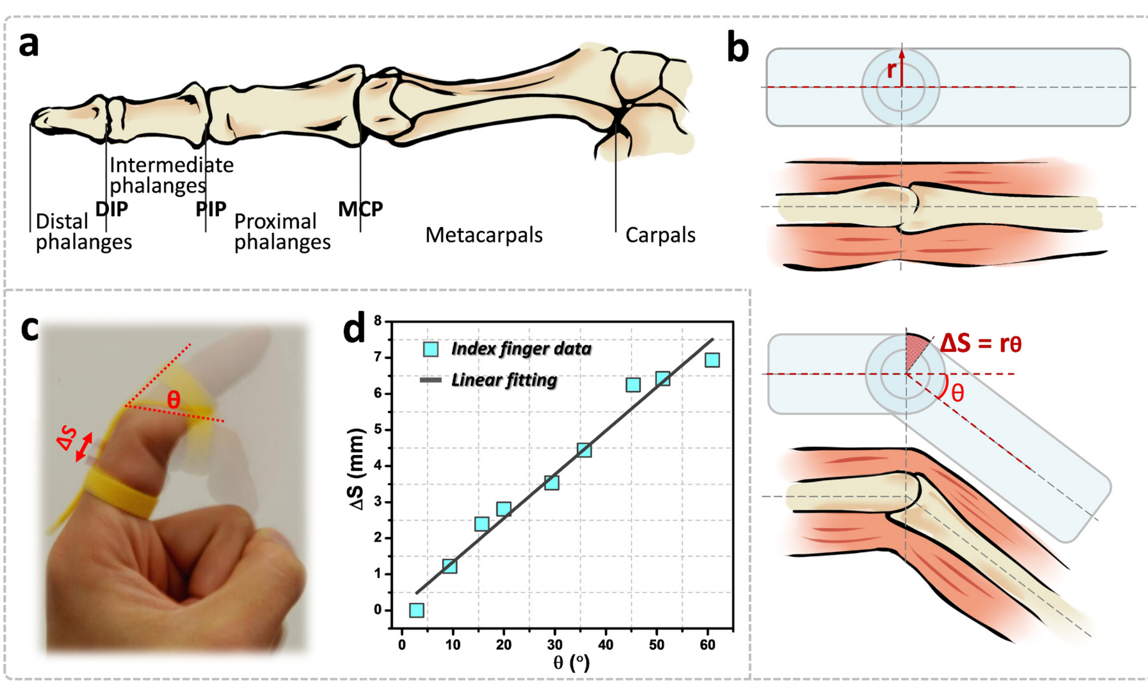

Fig. 2. Physiological basis for human-robot joint motion mapping via jmTQS. (a) The skeleton of human finger. (b)The theoretical hinge model to simulate hinge joint's flexion and extension. (c) and (d) The experimental model to verify the linear relationship between the rotation angle and the tensile displacement at the finger joint.

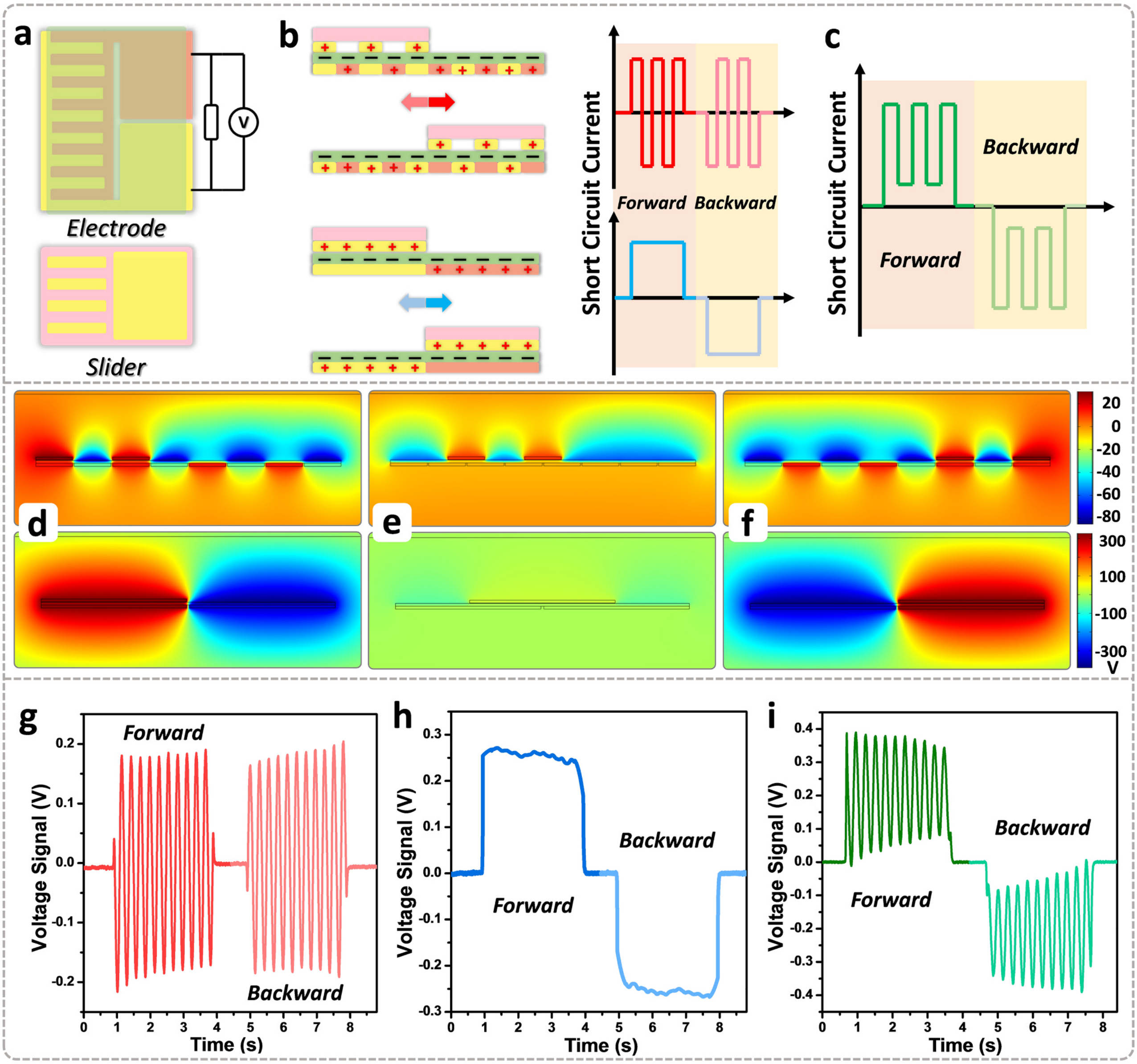

Fig. 3. Operating principle of the coupled freestanding jmTQS. (a) and (b) Schematics of the operation mechanism of the grating-interdigitated freestanding part and the block freestanding part. (c) Schematics of output signal of the coupled circuit. (d-f) Potential simulation by COMSOL to elucidate the working principle. (g-i) Real signals detected from the grating-interdigitated freestanding part, the block freestanding part, and the coupled circuit.

measurement. Fig. 3g-h show the real signals detected from the two independent parts and the coupled circuit. In a coupled mode, the durability of jmTQS has also been tested during 10,800 working circles (shown in Fig. S3). The stable output signal implies a long lifetime benefitting from the sponge foam structures which provide a better contact and reduce the abrasion caused by sliding. As a supplement, another structural scheme has been figured out to produce similar signals of a series of positive/negative pulses. The main point of design, the schematic drawing and the test data are illustrated in Fig. S4.

3.4. Performance of the jmTQS sensor

To quantitatively characterize the features of the jmTQS sensor, a home-made hinge component is employed to simulate the motion of the finger joint. A numerical controlled electric stepping motor is used to drive the hinge component to operate the jmTQS device. The test system is shown in Fig. 4a and Movie S1. To confirm that the pulse number can represent the finger joint's flexion-extension degree, the hinge component is driven by the stepping motor to rotate through different angles ($\Delta\theta$ = 20°, 40°, 60°) at a rotation speed of 20°/s, and then the corresponding sequences of pulses induced by the jmTQS (grating width = 0.7 mm) are recorded respectively, as illustrated in Fig. 4b. Counting the number of each sequence of pulses, we can find that the pulse number is linear to the rotation angle and it thus can represent the finger joint's flexion-extension degree. For $\Delta\theta$ = 60°, the missing of the half pulse at the end is caused by the dislocation of the gratings of the slider and the fixing part at the beginning which would not influence the control precision as long as the gratings are fine enough and the parameters are set well. To investigate if the rotation speed affects the pulse number, a piece of fabricated jmTQS (grating width = 0.7 mm) is fixed on the hinge model driven by the stepping motor to rotate through 60° at different rotation speed (60°/s, 40°/s, 20°/s). From Fig. 4c, we can conclude that although the pulse width change with the rotation speed, the total pulse number doesn't change at certain rotation degree, which means the jmTQS can stably sense the finger joint's flexion-extension degree and can directly reflect its

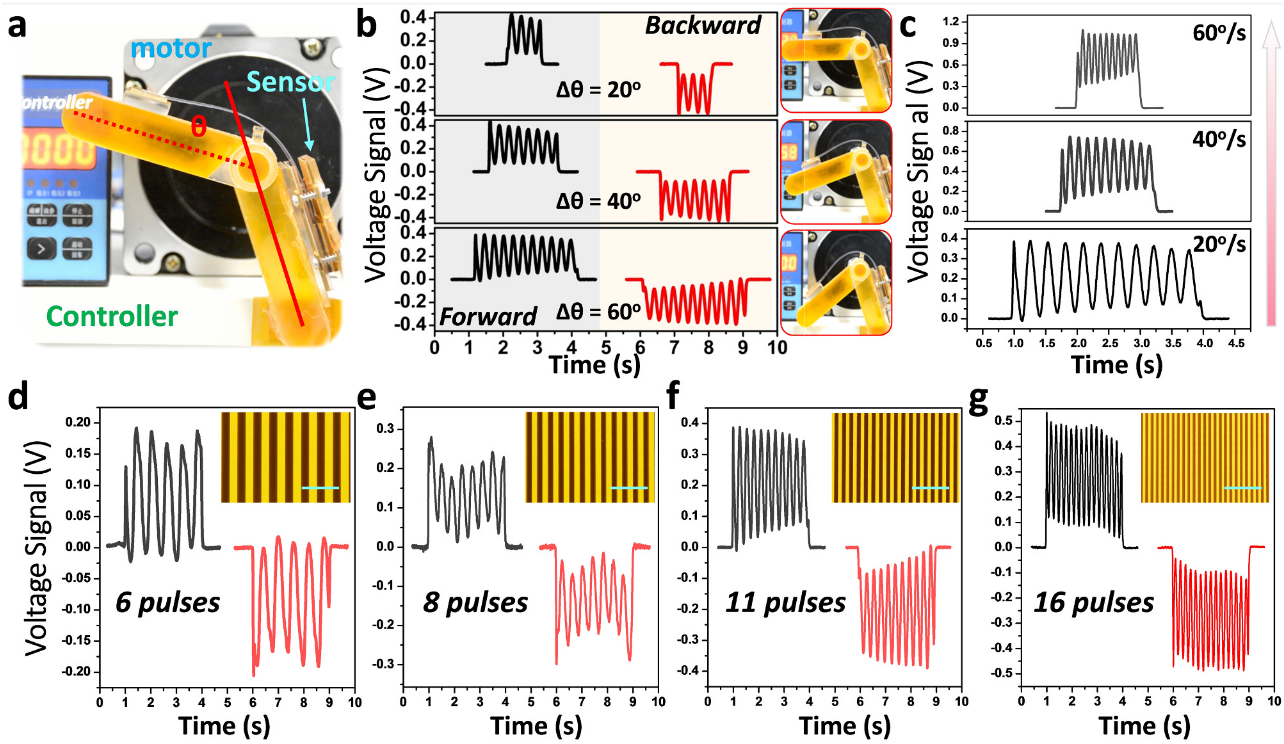

Fig. 4. Characterizing the performance of jmTQS. (a) The measurement model established with a programmable controller, a step motor, a single joint hinge component and the jmTQS. (b) The pulses generated from a jmTQS when the hinge model rotate through different angles (Δθ = 20°, 40°, 60°). The pulse number can approximately represent the relevant rotation angle. (c) The pulses produced from a jmTQS when the hinge model rotate through 60° at different rotation speed (60°/s, 40°/s, 20°/s). The rotation speed does not affect the number of pulses. (d-g) The pulses produced from the jmTQSs with different grating width (1.5 mm, 1.0 mm, 0.7 mm, 0.5 mm, scale bar: 7 mm) when the hinge model rotates through the same degree at a certain rotation speed.

moving speed. To improve the sensing accuracy, we fabricate jmTQSs with different grating width (1.5 mm, 1.0 mm, 0.7 mm, 0.5 mm) and record the output signals of these jmTQSs when the hinge component rotates through the same degree (60°) at a certain rotation speed (20°/s). From Fig. 4d-g, we can find that finer grating segments induce more pulses corresponding to a certain rotation degree which will bring better accuracy and real-time response when applied to robotic hands control. Furthermore, the minimum resolution angle of the fabricated jmTQSs is 3.8° (60°/16 pulses, see Fig. 4g), which tallies with the theoretic value by the hinge model. More details can be referred to Table S1.

3.5. Demonstration in synchronous robotic control

On the basis of the advantages of the jmTQS demonstrated above in directly sensing the finger joint's flexion-extension degree/speed, we develop a human-robotic hand synchronous action system to illustrate a controlling robotic hand via the intuitionistic mapping from jmTQS. Fig. 5a is the prospect of a natural interface between the human and robot. The robotic hand synchronous control system is developed on LabVIEW platform (National Instruments Corporation), as shown in Fig. 5b. At present, two channels (the index finger and the middle finger) are illustrated to show controlling a commercial robotic hand (LOBOT uhand, Shenzhen Hiwonder Technology Co., Ltd.) via jmTQS's direct sensing of human gesture. The pulses on the screen are induced by the jmTQSs worn on a subject's index finger and middle finger (as demonstrated in Fig. 5c). The enlarged picture of these signals indicates the flexion/extension action of the index finger, the middle finger, and both fingers. The minor crosstalk between the channels can be excluded by threshold settings. Then, the commercial robotic hand is connected to the computer through serial port and thus a real-time synchronous control of the robotic hand is achieved. The process flow of the whole robotic hand synchronous control system is illustrated in Fig. S5. Fig. 5d demonstrates performing a victory v-sign with the index finger and middle finger in an initialized state of complete flexion of five fingers. Fig. 5e and Fig. 5f demonstrate grasping one object via single-finger's control signal. This mode is realized through certain programming and may play an important role in disability assistance. More detail information can be referred to Movie S2–S3. Starting with an initialization for synchronizing the robotic hand and human hand, and to plus/minus a certain step value on the basis of the initial position value according to the positive/negative pulses induced by the jmTQS, the finger joint's angular position can be determined by absolute value and the intuitionistic human-robotic hand two-dimensional motion mapping can be preserved in the following operating course. Furthermore, via this sensing principle, the synchronous control can recover at any breakpoint in the flexion-extension process.

4. Conclusion

In summary, we have demonstrated a new kind of human-robotic hand intuitionistic motion sensing and control protocol by developing a finger-wearable TENG sensor to quantitatively detect the finger joint's flexion-extension degree, speed and direction. By counting the pulse number in unit time and signing the positive/negative peak to characterize flexion/extension, the finger joint's angular position can be located as a value on the basis of the initial position value and the intuitionistic mapping between the human hand and robotic hand can be built. Therefore, the amount of complex algorithms used in this domain can be greatly reduced. Furthermore, the jmTQS style can be applied in sensing other similar joint's movement and thus plays a more important role in the human-robot interface. To achieve a more excellent sensing accuracy and ultra-compact device, photoetching or ebeam technology can be adopted in creating gratings. And taking the finger joints' combined action in consideration, the one joint's model can be applied in the two other joints to study the motion law of finger

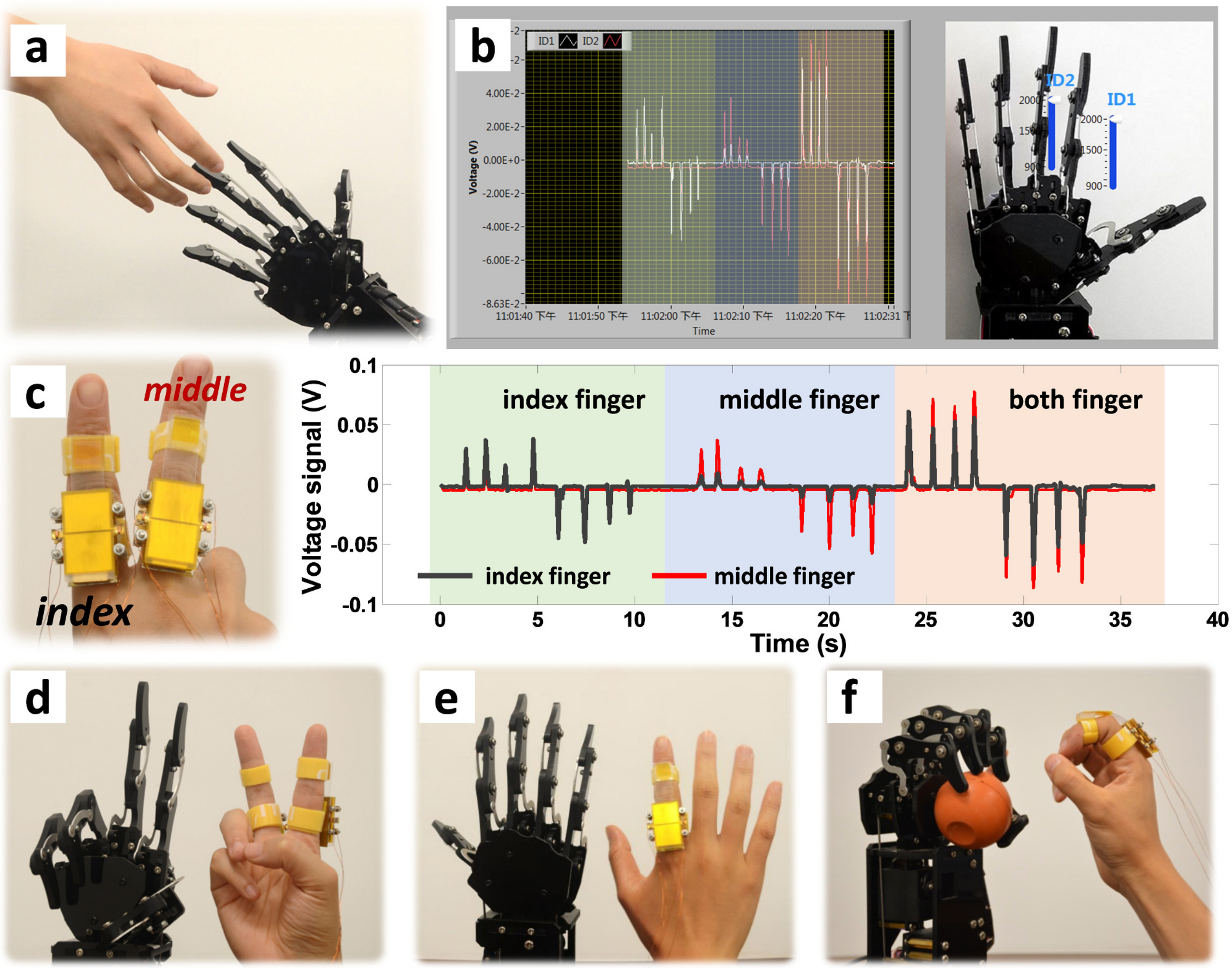

Fig. 5. Human-robot joint motion mapping via jmTQS and its application. (a) Prospect of the natural interface between human and robot. (b) Demonstration of the interface for controlling the robot hand via signal from jmTQS. (c) The control signals from jmTQSs worn on the index finger and the middle finger. Counting the pulse number in unit time and signing the positive/negative peak can accurately detect the flexion-extension degree/speed of each finger. (d) An example of performing the victory v-sign with two fingers. (e) and (f) Demonstration of grasping one object via single-finger's control signal with certain programming.

action. Then, we can achieve a more natural, high-precision and real-time synchronous movement of the human-robot.

Acknowledgements

Authors appreciate the help of Xiaozhi Wu, Wencheng Wang, Shiqin Dai and Xia Lin with the hinge model verification, schematic drawings and language correction. Research was supported by Minister of Science and Technology (2016YFA0202704), NSFC (51572040, 51772036), Science Challenge Project (No.TZ2016003), the Natural Science Foundation of Chongqing (cstc2017jcyjAX0307), the Fundamental Research Funds for the Central Universities (106112017CDJXY300002, 2018CDJDWL0011, 2018CDXYWU0025). Specially thanks to Luqiao Feng, a middle school student, who has actively participated in the researches of our group, including the fabrication of the triboelectric nanogenerator device.

Appendix B. Supporting information

Supplementary data associated with this article can be found in the online version at doi:10.1016/j.nanoen.2018.10.044.

References

[1] G.-Z. Yang, J. Bellingham, P.E. Dupont, P. Fischer, L. Floridi, R. Full, N. Jacobstein, V. Kumar, M. McNutt, R. Merrifeld, B.J. Nelson, B. Scassellati, M. Taddeo, R. Taylor, M. Veloso, Z.L. Wang, R. Wood, Sci. Rob. 3 (2018) eaar7650.
[2] N. Jacobstein, J. Bellingham, G.-Z. Yang, Sci. Rob. 2 (2017) eaan5594.
[3] L. Gallo, A.P. Placitelli, M. Ciampi, Proc. Comput. Based Med. Syst. Engl. 10 (2011) 1–6.
[4] M. Wang, W.Y. Chen, X.D. Li, Measurement 94 (2016) 734–744.
[5] T. D'Orazio, R. Marani, V. Renò, G. Cicirelli, Image Vis. Comput. 52 (2016) 56–72.
[6] M. Khezri, M. JahedA, IEEE Trans. Ind. Electron. 58 (2011) 1952–1960.
[7] J.W. Jeong, W.H. Yeo, A. Akhtar, J.J.S. Norton, Y.J. Kwack, S. Li, S.Y. Jung, Y. Su, W. Lee, J. Xia, Adv. Mater. 25 (2013) 6839–6846.
[8] N. Alves, T. Chau, Proc. Eng. Med. Biol. Soc. Argent. (2010) 3531.
[9] P.G. Jung, G. Lim, S. Kim, K. Kong, IEEE Trans. Ind. Inform. 11 (2017) 485–494.
[10] S. Alavi, D. Arsenault, A. Whitehead, Sensors 16 (2016) 605.
[11] P. Lukowicz, F. Hanser, C. Szubski, W. Schobersberger, Proc. Pervasive Comput., Irel. 3698 (2006) 101–116.
[12] J. Zhong, Q. Zhong, G. Chen, B. Hu, S. Zhao, X. Li, N. Wu, W. Li, H. Yu, J. Zhou, Energy Environ. Sci. 9 (2016) 3085–3091.
[13] Q. Zhong, J. Zhong, X. Cheng, X. Yao, B. Wang, W. Li, N. Wu, K. Liu, B. Hu, J. Zhou, Adv. Mater. 27 (2015) 7130–7136.
[14] D.-H. Kim, N. Lu, R. Ma, Y.-S. Kim, R.-H. Kim, S. Wang, J. Wu, S.M. Won, H. Tao, A. Islam, K.J. Yu, T.-i. Kim, R. Chowdhury, M. Ying, L. Xu, M. Li, H.-J. Chung, H. Keum, M. McCormick, P. Liu, Y.-W. Zhang, F.G. Omenetto, Y. Huang, T. Coleman, J.A. Rogers, Science 333 (2011) 838.
[15] W.H. Yeo, Y.S. Kim, J. Lee, A. Ameen, L. Shi, M. Li, S. Wang, R. Ma, S.H. Jin, Z. Kang, Y. Huang, J.A. Rogers, Adv. Mater. 25 (2013) 2773–2778.
[16] N. Wu, X. Cheng, Q. Zhong, J. Zhong, W. Li, B. Wang, B. Hu, J. Zhou, Adv. Funct. Mater. 25 (2015) 4788–4794.

[17] J. Xu, S. Wang, G.-J.N. Wang, C. Zhu, S. Luo, L. Jin, X. Gu, S. Chen, V.R. Feig, J.W.F. To, S. Rondeau-Gagné, J. Park, B.C. Schroeder, C. Lu, J.Y. Oh, Y. Wang, Y.-H. Kim, H. Yan, R. Sinclair, D. Zhou, G. Xue, B. Murmann, C. Linder, W. Cai, J.B.H. Tok, J.W. Chung, Z. Bao, Science 355 (2017) 59.
[18] K.C. Pradel, W. Wu, Y. Ding, Z.L. Wang, Nano Lett. 14 (2014) 6897–6905.
[19] Y.-C. Lai, J. Deng, S.L. Zhang, S. Niu, H. Guo, Z.L. Wang, Adv. Funct. Mater. 27 (2017) 1604462.
[20] K. Dong, J. Deng, W. Ding, A.C. Wang, P. Wang, C. Cheng, Y.-C. Wang, L. Jin, B. Gu, B. Sun, Z.L. Wang, Adv. Energy Mater. 8 (2018) 1801114.
[21] T. Bu, T. Xiao, Z. Yang, G. Liu, X. Fu, J. Nie, T. Guo, Y. Pang, J. Zhao, F. Xi, C. Zhang, Z.L. Wang, Adv. Mater. 30 (2018) e1800066.
[22] Y. Fang, X. Wang, S. Niu, S. Li, Y. Yin, K. Dai, G. Zhang, L. Lin, Z. Wen, H. Guo, Sci. Adv. 2 (2016) e1501624.
[23] R. Cao, X. Pu, X. Du, W. Yang, J. Wang, H. Guo, S. Zhao, Z. Yuan, C. Zhang, C. Li, Z.L. Wang, ACS Nano 12 (2018) 5190–5196.
[24] J. Chen, J. Yang, Z. Li, X. Fan, Y. Zi, Q. Jing, H. Guo, Z. Wen, K.C. Pradel, S. Niu, ACS Nano 9 (2015) 3324–3331.
[25] X. Pu, M. Liu, X. Chen, J. Sun, C. Du, Y. Zhang, J. Zhai, W. Hu, Z.L. Wang, Sci. Adv. 3 (2017) e1700015.
[26] G. Zhu, B. Peng, J. Chen, Q. Jing, Z.L. Wang, Nano Energy 14 (2015) 126–138.
[27] H. Guo, Q. Leng, X. He, M. Wang, J. Chen, C. Hu, Y. Xi, Adv. Energy Mater. 5 (2015) 1400790.
[28] H. Guo, M.H. Yeh, Y.C. Lai, Y. Zi, C. Wu, Z. Wen, C. Hu, Z.L. Wang, ACS Nano 10 (2016) 10580–10588.
[29] Z. Wen, M.H. Yeh, H. Guo, J. Wang, Y. Zi, W. Xu, J. Deng, L. Zhu, X. Wang, C. Hu, Sci. Adv. 2 (2016) e1600097.
[30] X. Pu, H. Guo, J. Chen, X. Wang, Y. Xi, C. Hu, Z.L. Wang, Sci. Adv. 3 (2017) e1700694.
[31] H. Guo, X. Pu, J. Chen, Y. Meng, M.-H. Yeh, G. Liu, Q. Tang, B. Chen, D. Liu, S. Qi, C. Wu, C. Hu, J. Wang, Z.L. Wang, Sci. Rob. 3 (2018) eaat2516.
[32] W. Gao, S. Emaminejad, N. Hyy, S. Challa, K. Chen, A. Peck, H.M. Fahad, H. Ota, H. Shiraki, D. Kiriya, D.-H. Lien, G.A. Brooks, R.W. Davis, A. Javey, Nature 529 (2016) 509–514.
[33] Y. Wu, Q. Jing, J. Chen, P. Bai, J. Bai, G. Zhu, Y. Su, Z.L. Wang, Adv. Funct. Mater. 25 (2015) 2166.
[34] Y.S. Zhou, G. Zhu, S. Niu, Y. Liu, P. Bai, Q. Jing, Z.L. Wang, Adv. Mater. 26 (2014) 1719–1724.
[35] J. Chen, X. Pu, H. Guo, Q. Tang, L. Feng, X. Wang, C. Hu, Nano Energy 43 (2018) 253–258.
[36] G. Figliolini, M. Ceccarelli, Robotica 20 (2002) 13–22.
[37] C.L. Taylor, R.J. Schwarz, Artif. Limbs 2 (1955) 22.

Xianjie Pu received her B.S. degree in Biomedical Engineering from Chongqing University in 2008 and M.S. degree in Biomedical Engineering from UESTC in 2011. She has been a faculty member of TMMU (2011–2014) and CQU (2014-). She is currently pursuing the Ph.D. degree with the Department of Applied Physics, CQU. Her current interests include self-powered sensors, systems and applications based on nanogenerators.

Hengyu Guo received his B. S. and Ph.D. degree in Applied Physics from Chongqing University, China. Now he is a postdoctoral fellow in Beijing Institute of Nanoenergy and Nanosystems, Chinese Academy of Sciences, China. His current research interest is triboelectric nanogenerator based energy and sensor systems.

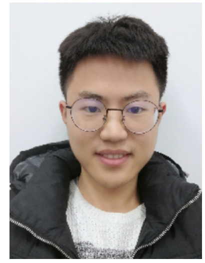

Qian Tang received his B.S. in Physics (2016) from China West Normal University. Now, he is a postgraduate student in Chongqing University. Currently, his research interests are mainly focused on energy harvesting for self-powered system.

Jie Chen received her B. S. degree in Applied Physics from Chongqing University, China in 2015. Now she is a Ph.D. candidate in the field of Physics, Chongqing University. Her current research interest is triboelectric nanogenerator.

Li Feng received her B.S. in Physics (2016) from China West Normal University. Now, she is a postgraduate student in Chongqing University. Currently, her research interests are mainly focused on triboelectric nanogenerator.

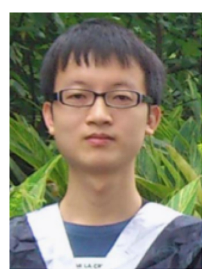

Guanlin Liu received his B.S. degree in Applied Physics (2014) from Chongqing University. Now, he is a Ph.D. student in Chongqing University. His research interests are mainly focused on nanogenerator.

Xue Wang received her Ph. D. degree in Condensed Matter Physics in 2012 form Chongqing University, China. Now, she is an associate professor of Chongqing University. Her research interests are related to the designs and synthesis of functional nanomaterials for energy conversion and storage, including nanogenerators and supercapacitors.

Yi Xi received her Ph.D. in 2010 in Physics from Chongqing University, China. Now she is an associate professor at Chongqing University, China. Her main research interests focus on the fields of piezoelectric, triboelectric nanogenerators for energy harvesting and supercapacitors for energy storage, driving some personal electronic devices.

Chenguo Hu Chenguo Hu is a professor of physics in Chongqing University and the director of Key Lab of Materials Physics of Chongqing Municipality. She received her Ph.D. from Chongqing University in 2003. Her research interests include the investigation of morphology and size dependent physical and chemical properties of nanomaterials, and design and fabrication of electronic devices, such as nanogenerators and self-powered sensors.

Zhong Lin Wang is a Hightower Chair and Regents's Professor at Georgia Tech. He is also the Chief scientist and Director for the Beijing Institute of Nanoenergy and Nanosystems, Chinese Academy of Sciences. His discovery and breakthroughs in developing nanogenerators establish the principle and technological road map for harvesting mechanical energy from environmental and biological systems for powering personal electronics. He coined and pioneered the field of piezotronics and piezo-phototronics by introducing piezoelectric potential gated charge transport process in fabricating new electronic and optoelectronic devices.